AD750110

EDGEWOOD ARSENAL
TECHNICAL REPORT

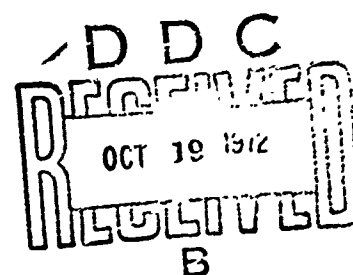## EATR 4660

A LIGHT SCATTERING TECHNIQUE
FOR STUDYING BROWNIAN MOTION

by

M. E. Milham

September 1972

DDC
RECEIVED
OCT 19 1972
B

DEPARTMENT OF THE ARMY
EDGEWOOD ARSENAL
Directorate of Development and Engineering
Edgewood Arsenal, Maryland 21010

37

Distribution Statement

Approved for public release; distribution unlimited.

Disclaimer

The findings in this report are not to be construed as an official Department of the Army position unless so designated by other authorized documents.

Disposition

Destroy this report when no longer needed. Do not return it to the originator.

DOCUMENT CONTROL DATA - R & D

(Security classification of title, body of abstract and indexing annotation must be entered when the overall report is classified)

1. ORIGINATING ACTIVITY (Corporate author)	2a. REPORT SECURITY CLASSIFICATION
CO, Edgewood Arsenal ATTN: SMUEA-DE-MM Edgewood Arsenal, Maryland 21010	UNCLASSIFIED
	2b. GROUP NA

3. REPORT TITLE

A LIGHT SCATTERING TECHNIQUE FOR STUDYING BROWNIAN MOTION

4. DESCRIPTIVE NOTES (Type of report and inclusive dates)

This work was started in September 1970 and completed in May 1971.

5. AUTHOR(S) (First name, middle initial, last name)

Merrill E. Milham

6. REPORT DATE	7a. TOTAL NO. OF PAGES	7b. NO. OF REFS
September 1972	37	30

8a. CONTRACT OR GRANT NO.	9a. ORIGINATOR'S REPORT NUMBER(S)
b. PROJECT NO.	EATR 4660
Task No. 1B562602A081	9b. OTHER REPORT NO(S) (Any other numbers that may be assigned this report)
d.	

10. DISTRIBUTION STATEMENT

Approved for public release; distribution unlimited.

11. SUPPLEMENTARY NOTES	12. SPONSORING MILITARY ACTIVITY
	NA

13. ABSTRACT

The purpose of this work is to study the light scattered from a simple statistical medium that consisted of a monodispersed ensemble of spherical, Brownian particles. The light from a helium-neon laser operating at a wavelength of 632.8 nm is scattered from a dilute water suspension of the particles, which are polystyrene spheres of diameter 0.557 μm. The spectrum of the scattered light is a very narrow Lorentzian whose half width at half height is related to the diffusion constant of the particles. The scattered light is allowed to fall on a photomultiplier tube, and the times between successive photocounts are determined. The distribution of these time intervals is not random for times on the order of, or less than, the coherence time of the light. The probability of counting two pulses under such conditions is greater than could be expected for random events. The "bunching" of the photocounts (photons) is related to the spectral shape of the scattered light. An experiment that employs the technique of pulse interval analysis to analyze the scattered light spectrum is described in detail. The results of this experiment yielded a spectral linewidth that is caused not only by the diffusive motion, but also by the convective motion of the particles. This determination of the linewidth was found to be in agreement with previous experimental results.

14. KEYWORDS

Aerosols	Laser	Photon punching
Brownian motion	Correlation function	Pulse interval analysis
Light scattering	Wiener-Khintchine theorem	Particle sizing

DD FORM 1473 REPLACES DD FORM 1473, 1 JAN 64, WHICH IS OBSOLETE FOR ARMY USE.

UNCLASSIFIED
Security Classification

I

EDGEWOOD ARSENAL TECHNICAL REPORT

EATR 4660

A LIGHT SCATTERING TECHNIQUE FOR STUDYING BROWNIAN MOTION

by

M. E. Milham

Munitions Systems Division

September 1972

Task 1B562602A081

DEPARTMENT OF THE ARMY
EDGEWOOD ARSENAL
Directorate of Engineering and Development
Edgewood Arsenal, Maryland 21010

1

FOREWORD

Acknowledgment

DIGEST

The purpose of this work is to study the light scattered from a simple statistical medium that consisted of a monodispersed ensemble of spherical, Brownian particles. The light from a helium-neon laser operating at a wavelength of 632.8 nm is scattered from a dilute water suspension of the particles, which are polystyrene spheres of diameter 0.557 μm. The spectrum of the scattered light is a very narrow Lorentzian whose half width at half height is related to the diffusion constant of the particles. The scattered light is allowed to fall on a photomultiplier tube, and the times between successive photocounts are determined. The distribution of these time intervals is not random for times on the order of, or less than, the coherence time of the light. The probability of counting two pulses under such conditions is greater than could be expected for random events. This "bunching" of the photocounts (photons) is related to the spectral shape of the scattered light. An experiment that employs the technique of pulse interval analysis to analyze the scattered light spectrum is described in detail. The results of this experiment yielded a spectral linewidth that is caused not only by the diffusive motion, but also by the convective motion of the particles. This determination of the linewidth was found to be in agreement with previous experimental results.

3

CONTENTS

LIST OF FIGURES

A LIGHT SCATTERING TECHNIQUE FOR STUDYING BROWNIAN MOTION

I. INTRODUCTION.

Brownian motion is a topic of considerable importance in the study of aerosol mechanics.[1] Many diverse aerosol phenomena involve Brownian motion. Among these are: (1) deposition of aerosol particles from a stationary gas; (2) diffusion of aerosols in laminar flow; (3) filtration; (4) deposition of aerosols in the respiratory system; (5) absorption of aerosols by bubbling; and (6) coagulation of aerosols. Also, the Brownian motion of aerosols can be used as a particle sizing method.[1]

There is a 50-year tradition of extracting physical data from light scattering experiments. The advent of lasers with their very narrow linewidths and high coherence has revolutionized nearly all aspects of light scattering. The technique of studying Brownian motion by means of light scattering is one area that has been opened up by the development of the laser. Although this technique has so far been applied only to the motion of particles in liquid media, the application of such a technique to aerosols appears very promising.

The purpose of this paper is to study the light scattered from a simple statistical medium that consists of a monodispersed ensemble of spherical, Brownian particles. The light from a helium-neon laser operating at a wavelength of 632.8 nm is scattered from a dilute water suspension of the particles, which are polystyrene spheres of diameter 0.557 μm (see figure 1). The spectrum of the scattered light is a very narrow Lorentzian whose half width at half height is related to the diffusion constant of the particles.
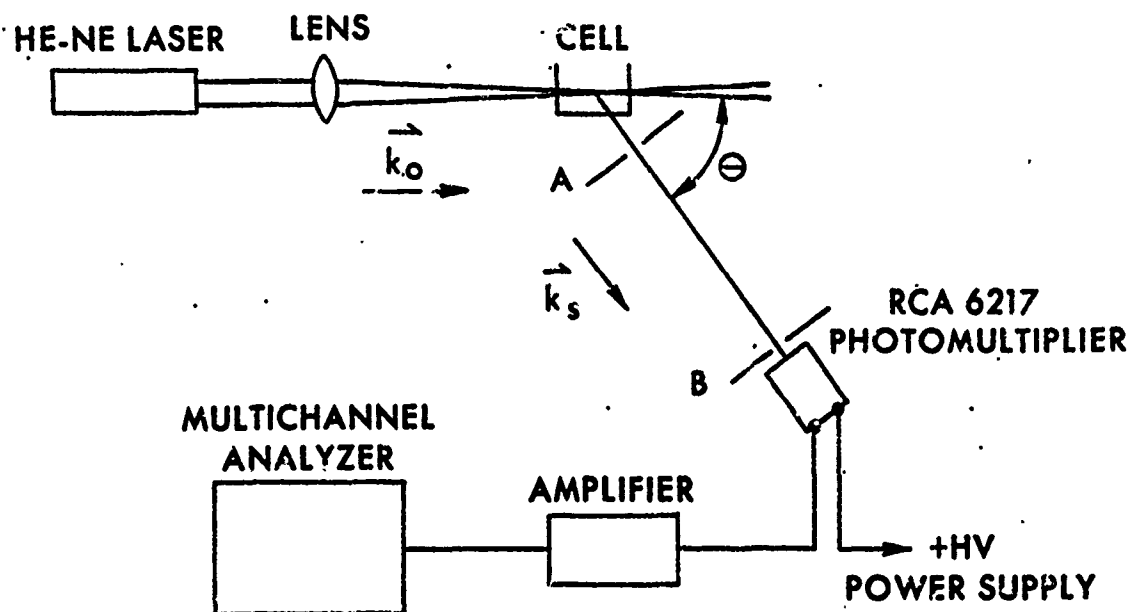

Figure 1. Experimental Arrangement

---

[1] Fuchs, N. A. The Mechanics of Aerosols. The Macmillan Company, New York, New York. 1964.

The scattered light is allowed to fall on a photomultiplier tube, and the times between successive photocounts are determined. The distribution of these time intervals is not random for times on the order of, or less than, the coherence time of the light. The probability of counting two pulses under such conditions is greater than could be expected for random events. This "bunching" of the photocounts (photons) is related to the spectral shape of the scattered light.

In fact, the bunching phenomenon will be used to determine the spectral linewidth of the scattered light. Such a pulse interval technique is a very attractive method of studying these spectra because as the linewidth narrows, there is a corresponding decrease in the required time resolution.

II. BROWNIAN MOTION.

The phenomenon that we now know as Brownian motion was observed for the first time in 1827 by the botanist Robert Brown. He observed that material particles dispersed in a liquid execute an incessant, irregular, and randomly directed motion. Subsequent studies by several investigators showed that there was no apparent external cause for these motions. At the beginning of this century, Einstein and Smoluchowski were able to show that Brownian motion is a direct manifestation of thermal agitation;[2,3] that is, the motions of the particles are produced by fluctuations in the collisions with the molecules of the surrounding fluid. In their approach Brownian motion was treated as a problem in random walks.

In the random walk approach, a Brownian particle undergoes a sequence of displacements, $\vec{s}_1$, $\vec{s}_2$, $\cdots$, $\vec{s}_i$, because of collisions with the fluid molecules. These displacements are Markovian in nature because the magnitude and direction of each displacement are independent of all the preceding ones. However, the probability that the displacement, $\vec{s}_i$, lies between $\vec{s}_i$ and $\vec{s}_i + d\vec{s}_i$ is governed by some distribution function, $p_i(\vec{s}_i)$. The total displacement, $\vec{S}$, after a number of such displacements is given by

$$\vec{S} = \sum_i \vec{s}_i \tag{1}$$

The solution to the problem is given by determining the probability $P(\Delta\vec{S},\Delta t)$ that the particle acquires a net displacement $\Delta\vec{S}$ in time Δt.

If Δt denotes an interval of time long enough for a particle to suffer a large number of displacements but still short enough for the net mean square increment $\langle|\Delta\vec{S}|^2\rangle$ to be small, then it can be shown that[2-4]

$$P(\vec{r},t|\vec{r}_0,t_0) = \frac{1}{(4\pi D\Delta t)^{3/2}} e^{-|\vec{r}-\vec{r}_0|^2/4D\Delta t} \tag{2}$$

where

$$\Delta\vec{S} = \vec{r} - \vec{r}_0$$

[2]Einstein, A. Investigations on the Theory of the Brownian Movement. ed R. Furth. Dover, New York, New York. 1956.

[3]Chandrasekhar, S. Stochastic Problems in Physics and Astronomy. Rev. Mod. Phys. *15*, 1 (1943).

[4]Wang, M. C., and Uhlenbeck, G. E. On the Theory of the Brownian Motion II, Rev. Mod. Phys. *17*, 323 (1945).

since

$\vec{r}_0$ = position vector of the particle at time $t = t_0$

$\vec{r}$ = position vector of the particle at time t

and

$\Delta t = t - t_0$

The constant D is known as the diffusion constant and is defined for a spherical particle that obeys Stokes law as

$$D = \frac{kT}{3\pi\eta d} \tag{3}$$

where

k = the Boltzman constant

T = temperature

η = viscosity of the liquid

d = particle diameter

Substituting equation 2 into the definition of the mean square displacement, we get that

$$\langle |\vec{r}-\vec{r}_0|^2 \rangle = (4\pi D\Delta t)^{-3/2} \int_{-\infty}^{\infty} |\vec{r}-\vec{r}_0|^2 P(\vec{r},t|\vec{r}_0,t_0)d\vec{r} = 6D\Delta t \tag{4}$$

Also, by definition

$$\langle |\vec{r}-\vec{r}_0|^2 \rangle = \langle (x-x_0)^2 \rangle + \langle (y-y_0)^2 \rangle + \langle (z-z_0)^2 \rangle \tag{5}$$

And because the liquid medium is homogeneous and isotropic

$$\langle (x-x_0)^2 \rangle = 1/3 \langle |\vec{r}-\vec{r}_0|^2 \rangle = 2D\Delta t \tag{6}$$

The equation for the distribution of displacements (equation 2) and the equation for the mean square displacement (equation 6) have both been verified experimentally by Perrin.[2,3]

III. LIGHT SCATTERING.

Consider the cell (see figure 1) to be filled with a suspension containing M identical light scattering particles. The incident laser light is polarized perpendicular to the scattering plane, and the light scattered at an angle θ is observed at a distance R from the illuminated cell.

Each of the particles is subjected to an incident field, $\vec{E}_0 e^{i(\vec{k}_0 \cdot \vec{r} - \omega_0 t)}$, where $\vec{k}_0$ is the wave vector of the incident laser beam, and ω_0 is the corresponding angular frequency. If the

9

number density of the particles is low enough to preclude any secondary scattering, then the total scattered field at $\vec{R}$ is given by

$$\vec{E}(t) = \sum_{j=1}^{M} \vec{E}_0^j e^{i[\phi_j(t) - \omega_0 t]} \tag{7}$$

The phase factor, $\phi_j(t)$, contains information about the temporal variation of the position of the particle, $\vec{r}_j$. To see this explicitly, consider the situation shown in figure 2. The path of the ray through the point, r_j, is longer than the path through the point, $\vec{r}_0$, by the sum of the distances a and b, where

$$a = |\vec{r}_j - \vec{r}_0| \cos \eta_0 \tag{8}$$

and

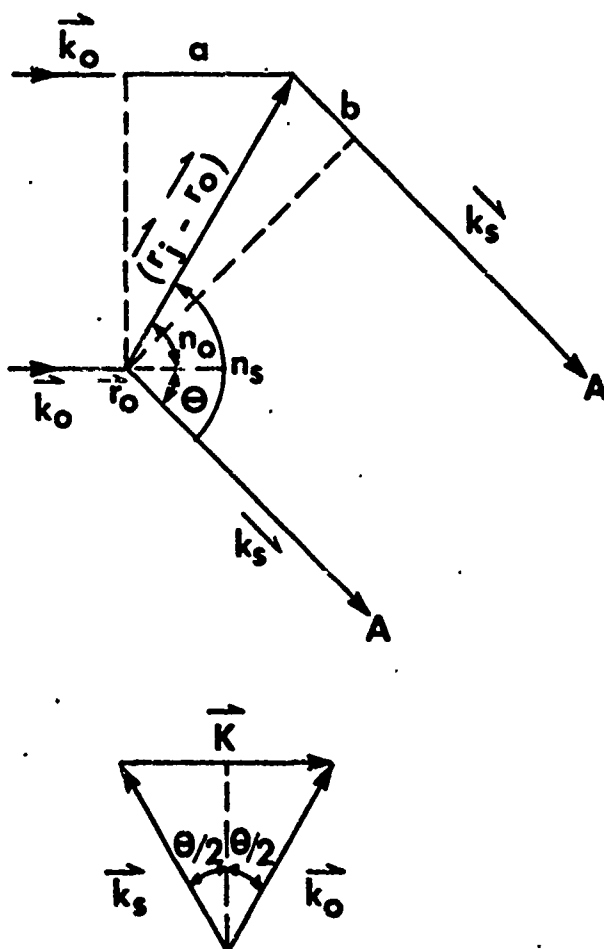$$b = -|\vec{r}_j - \vec{r}_0| \cos \eta_s \tag{9}$$

Figure 2. Scattering Geometry

10

Therefore, the phase factor is just

$$\phi_j = |\vec{r}_j - \vec{r}_0| \cos \eta_0 |\vec{k}_0| - |\vec{r}_j - \vec{r}_0| \cos \eta_s |\vec{k}_s| = (\vec{k}_0 - \vec{k}_s) \cdot (\vec{r}_j - \vec{r}_0) \qquad (10)$$

For convenience let us define the scattering vector,

$$\vec{K} = \vec{k}_0 - \vec{k}_s \qquad (11)$$

For particles of velocity, $v \ll C$, we have that

$$|\vec{k}_0| \approx |\vec{k}_s| \qquad (12)$$

and from figure 2

$$|\vec{K}| = 2|\vec{k}_0| \sin \theta/2 = \frac{4\pi n_0}{\lambda} \sin \theta/2 \qquad (13)$$

where

n_0 = refractive index of the medium

λ = wavelength of the laser radiation in vacuo

In terms of the scattering vector, $\vec{K}$, the phase factor is given by

$$\phi_j(t) = \vec{K} \cdot (\vec{r}_j - \vec{r}_0) \qquad (14)$$

From this relationship we see that $\phi_j(t)$ changes only if the particle has a displacement component along $\vec{K}$. Any displacement of the particle normal to $\vec{K}$ leaves $\phi_j(t)$ unaltered. The phase factor is, of course, a random variable because it depends upon $\vec{r}_j$.

The quantity $-|\vec{E}_0'|$ depends, in general, on the size and shape of the scattering particle. If the particles are spheres that are small enough to meet the Rayleigh criterion, $d \ll \lambda$, and if $(m-1) \ll 1$, then[5]

$$|\vec{E}_0'|_R = \frac{2\pi^3 d^3}{\lambda^2} \frac{e^{i(\vec{k}_s \cdot \vec{R})}}{|\vec{R}|} |\vec{E}_0| \sin \Psi (m-1) \qquad (15)$$

where

$|\vec{E}_0'|_R$ = magnitude of the electric field due to Rayleigh scattering

m = index of refraction of the particle relative to the medium

Ψ = the angle between the direction of $\vec{E}_0$ and the direction of propagation, $\vec{k}_s$, of scattered wave

[5]Clark, N. A., Lunacek, J. H., and Benedek, G. B. A Study of Brownian Motion Using Light Scattering. Amer. J. Phys. 38, 575 (1970).

11

If the light scattering particles are too large to satisfy the Rayleigh criterion, but they do satisfy the requirement that $(m - 1) \ll 1$ and the Rayleigh-Gans criterion, $kd/2(m - 1) \ll 1$, then each volume element of the particle gives Rayleigh (dipole) scattering that is independent of the other volume elements. The waves scattered in a given direction by all volume elements interfere because of their spatial distribution, and the total scattered field for a single particle is found by integration over the whole scatterer. Under these conditions it can be shown that[6]

$$|\vec{E}_0'|_{R\text{-}G} = |\vec{E}_0'|_R \left[i/V \int e^{i\vec{K}\cdot\vec{r}}dV \right] \qquad (16)$$

where $|\vec{E}_0'|_{R\text{-}G}$ is the magnitude of the electric field caused by Rayleigh-Gans scattering and for spherical particles

$$1/V \int e^{i\vec{K}\cdot\vec{r}}dV = \left(\frac{36\pi}{|\vec{K}|^3 d^3} \right)^{\frac{1}{2}} J_{3/2}(|\vec{K}|d/2) \qquad (17)$$

Equation 15 gives $|\vec{E}_0'|_R$ for the case of spheres.

The index of refraction for polystyrene spheres relative to water is 1.20 (sodium D line),[7] so that for particles of 0.557 μm diameter:

$$(m - 1) \approx 0.20 \qquad (18)$$

and

$$kd/2(m - 1) \approx 0.55 \qquad (19)$$

Therefore, it may be concluded that these particles are scatterers of the Rayleigh-Gans type.

Since $E(t)$ and $I(t) = |E(t)|^2$ depend upon the random phases of the waves scattered by each particle, it is impossible to predict the detailed temporal evolution of these quantities. However, such a random process can be characterized by quantities such as $\langle I(t) \rangle$, the average intensity, $\langle \vec{E}^*(t)\vec{E}(t + \tau) \rangle$, the correlation function for the field, and $\langle I(t)I(t + \tau) \rangle$, the correlation function for the intensity.[5,8] If the temporal fluctuations in $\vec{E}(t)$ and $I(t)$ are stationary, then the corresponding correlation functions depend only upon the time increment, τ. The spectrum, $Q(\omega)$, of such a random process is related to its correlation function by the Wiener-Khintchine theorem,[4,8]

$$Q(\omega) = 1/2\pi \int_{-\infty}^{\infty} G^{(1)}(\tau)e^{-i\omega\tau}d\tau \qquad (20)$$

where $G^{(1)}(\tau)$ is the correlation function $\langle G^*(t)G(t + \tau) \rangle$.

[6] Van De Hulst, H. C. Light Scattering by Small Particles. John Wiley & Sons, New York, New York. 1957.

[7] Ashley, L. E., and Cobb, C. M. Single Particle Scattering Functions for Latex Spheres in Water. J. Opt. Soc. Amer. 48, 261 (1958).

[8] Korn, G. A., and Korn, T. A. Mathematical Handbook for Scientists and Engineers. McGraw Hill, New York, New York. 1961.

The correlation function for the scattered field is

$$C^{(1)}(\tau) = \left\langle \sum_{j=1}^{M} \vec{E}_0^{'} e^{-i[\phi_j(t) - \omega_0 t]} \sum_{l=1}^{M} \vec{E}_0^{'} e^{i[\phi_l(t+\tau) - \omega_0(t+\tau)]} \right\rangle \qquad (21)$$

Because the particles move in such a way that the motion of any one particle is completely uncorrelated with the motion of any other particle, the cross terms ($j \neq l$) of this double summation may be eliminated. Furthermore, each of the M scatterers is identical so that the correlation function for the ensemble is just M times the single particle correlation function. Thus, with the aid of equation 14,

$$C^{(1)}(\tau) = M |\vec{E}_0^{'}|^2 \, e^{-i\omega_\bullet \tau} C_\phi(\tau) \qquad (22)$$

where

$$C_\phi(\tau) = \langle e^{i\vec{K} \cdot (\vec{r} - \vec{r}_0)} \rangle \qquad (23)$$

and

$$\vec{r} = \vec{r}(t + \tau)$$

$$\vec{r}_0 = \vec{r}(t)$$

The ensemble average indicated for $C_\phi(\tau)$ can be evaluated by integrating over the probability distribution, $P(\vec{r}, t + \tau | \vec{r}_0, t)$,

$$C_\phi(\tau) = \int_{-\infty}^{\infty} P(\vec{r}, t + \tau | \vec{r}_0, t) \, e^{i\vec{K} \cdot (\vec{r} - \vec{r}_0)} d\vec{r} \qquad (24)$$

The probability distribution $P(\vec{r}, t + \tau | \vec{r}_0, t)$ is given by equation 2 for a Brownian particle. Substituting equation 2 into equation 24 and evaluating the integral we get that

$$C_\phi(\tau) = e^{-D |\vec{K}|^2 |\tau|} \qquad (25)$$

and

$$C^{(1)}(\tau) = M |\vec{E}_0^{'}|^2 \, e^{-D |\vec{K}|^2 |\tau|} \, e^{-i\omega_\bullet \tau} \qquad (26)$$

The optical spectrum can then be calculated from the Wiener-Khintchine theorem

$$I(\omega) = M |\vec{E}_0^{'}|^2 / 2\pi \int_{-\infty}^{\infty} e^{i(\omega - \omega_\bullet)\tau} \, e^{-D |\vec{K}|^2 |\tau|} d\tau \qquad (27)$$

or

$$I(\omega) = M |\vec{E}_0^{'}|^2 \, \frac{D |\vec{K}|^2 / \pi}{(\omega - \omega_0)^2 + (D |\vec{K}|^2)^2} \qquad (28)$$

13

which is a Lorentzian centered at $\omega = \omega_0$ and with a half width at half maximum of

$$\delta\omega = D \mid \vec{K} \mid^2 \tag{29}$$

With the aid of equation 3 and the fact that $\lambda = 632.8$ nm, the linewidth for spherical particles in water at 20°C becomes[9]

$$\delta\omega = \frac{98 \pi \sin^2 \theta/2}{d} \tag{30}$$

where d = diameter of the spherical particles in μm. From the correlation function (equation 26) it can be seen that when τ substantially exceeds the time

$$\tau_c = 1 /D \mid \vec{K} \mid^2 = 1/\delta\omega \tag{31}$$

the scattered field approaches zero. This time, τ_c, is referred to as the coherence time. The expression for the coherence time (equation 31) can be validated formally from the definition[10]

$$\tau_c = \int_{-\infty}^{\infty} |C^{(1)}(\tau)|^2 \, d\tau \tag{32}$$

Thus, an important result, that the spectrum of the light scattered from a dilute suspension of particles undergoing translational diffusion is Lorentzian and contains information about the motion of the particles including the diffusion constant, has been reached. For the case of polystyrene spheres with diameters on the order of 10^{-1} μm, an extremely narrow linewidth, $\delta\nu \approx 10^2$ Hz, is predicted (equation 30). Thus, an analysis method is required that will resolve spectra that are too narrow for the usual spectroscopic techniques, which are, at best, able to resolve lines of width, $\delta\nu \approx 10^7$ Hz. Such methods are considered in the next section.

IV. SPECTRUM ANALYSIS.

As was pointed out in section III, the spectrum of the light scattered from a suspension of dilute polystyrene spheres necesitates a method of spectrum analysis that is more sensitive by a factor of $\approx 10^5$ over the usual dispersive spectroscopic methods. The interaction of light with a photoelectric detector provides the basis for two related techniques of successfully measuring such spectra: (1) by examining the photoelectron current spectrum produced by light beating; and (2) by using the statistical properties of individual photoelectrons.

A. Light Beating.

Light beating may be described as the mixing at a photocathode of two narrow band optical components to produce an a.c. component in the photocurrent at the optical difference frequency. The existence of this phenomenon was first demonstrated experimentally by Forrester, Gudmundsen, and Johnson in 1955.[11] Distributed optical spectra also can be resolved by this

[9]Cummins, H. Z., Knable, N., and Yeh, Y. Observation of Diffusion Broadening of Rayleigh Scattered Light. Phys. Rev. Lett. *12*, 150 (1964).

[10]Mandel, L., and Wolf, E. Coherence Properties of Optical Fields. Rev. Mod. Phys. *37*, 231 (1965).

[11]Forrester, A. T., Gudmundsen, R. A., and Johnson, F. O. Photoelectric Mixing of Incoherent Light. Phys. Rev. *99*, 1961 (1955).

method. Forrester[12] considered a distributed spectral line as a series of "slices" and found by a simple extension of the two-component case the beating between all possible pairs of slices. For a Lorentzian intensity distribution he showed that the power spectral density of the photocurrent is also a Lorentzian centered at $\omega = 0$ and with a doubled half width. Such a photocurrent spectrum may be Fourier analyzed with an electronic spectrum analyzer to obtain the pertinent spectral information.

B. Photoelectron Statistics.

The statistical distribution of individual photoelectrons emitted from a photocathode is intimately related to the incident optical spectrum. For incident light with a perfectly constant intensity, the probability, $p(n,T)$, of counting n photoelectrons in time T ($T \ll 1/\delta\nu$) is

$$p(n, T) = \langle n \rangle^n / n! e^{-\langle n \rangle} \tag{33}$$

which is a Poisson distribution with variance

$$\langle (\Delta n)^2 \rangle = \langle n \rangle \tag{34}$$

For monochromatic light scattered by a dilute suspension of scatterers, the scattered field, $\vec{E}(\vec{r},t)$, is a Gaussian random process[13] and for $T \ll 1/\delta\nu$

$$p(n, T) = \left[(1 + \langle n \rangle)(1 + 1/\langle n \rangle)^n \right]^{-1} \tag{35}$$

with variance

$$\langle (\Delta n)^2 \rangle = \langle n \rangle + \langle n \rangle^2 \tag{36}$$

These relationships (equations 33, 34, 35, and 36) illustrate the general situation in which the photocount distribution will depart from the Poisson form, and the variance of the number of counts is in excess of that given by Poisson statistics.[10] The nonrandom arrival of the photoelectrons is a manifestation of the characteristic bunching properties of photons. Several techniques by which the optical spectrum may be deduced from an analysis of photoelectron statistics have been reported.[14-18] The use of delayed photoelectron coincidence measurements to determine the linewidth[19-21] will be considered in detail below.

[12]Forrester, A. T. Photoelectric Mixing as a Spectroscopic Tool. J. Opt. Soc. Amer. *51*, 253 (1961).

[13]Cummins, H. Z., and Swinney, H. L. Progress in Optics. Vol VIII. ed E. Wolf. John Wiley & Sons, New York, New York. 1970.

[14]Jakeman, E., and Pike, E. R. The Intensity-Fluctuation Distribution of Gaussian Light. J. Phys. A, Proc. Phys. Soc. (London) *1*, 128 (1968).

[15]Mandel, L., and Wolf, E. Comments on a Paper by E. Jakeman and E. R. Pike, 'The Intensity-Fluctuation Distribution of Gaussian Light.' J. Phys. A, Proc. Phys. Soc. (London) *1*, 625 (1968).

[16]Jakeman, E., Oliver, C. J., and Pike, E. R. A Measurement of Optical Linewidth by Photon-Counting Statistics. J. Phys. A, Proc. Phys. Soc. (London) *1*, 406 (1968).

[17]Arrecchi, F. T., Berné, A., and Sona, A. Measurement of the Time Evolution of a Radiation Field by Joint Photocount Distributions. Phys. Rev. Lett. *17*, 260 (1966).

[18]Bédard, G. N-Fold Joint Photon Counting Distributions Associated with the Photoelection of Gaussian Light. Phys. Rev. *161*, 1304 (1967).

[19]Morgan, B. L., and Mandel, L. Measurement of Photon Bunching in a Thermal Light Beam. Phys. Rev. Lett. *16*, 1012 (1966).

[20]Phillips, D. T., Kleiman, H., and Davis, S. P. Intensity-Correlation Linewidth Measurement. Phys. Rev. *153*, 113 (1967).

[21]Pusey, P. N., and Goldburg, W. I. Temperature Dependence of Concentration Fluctuations in a Binary Liquid Mixture Using a Photon Correlation Method. Appl. Phys. Lett. *13*, 321 (1968).

The emission of an electron from an illuminated photosensitive surface is fundamentally a quantum mechanical process and has been so described by Glauber.[22] For the optical fields under consideration here, however, the semiclassical treatment of Mandel and Wolf[10] is entirely adequate.[13] This treatment considers the optical field at the photocathode to be specified by a real vector function

$$\vec{E}^{(r)}(\vec{r},\, t) = \int_{-\infty}^{\infty} \vec{V}(\vec{r},\, \omega)\, e^{-i\omega t}\, d\omega \tag{37}$$

Since $\vec{E}^{(r)}$ is real, $\vec{V}(\vec{r},\, \omega) = \vec{V}^*(\vec{r},\, \omega)$, and $\vec{E}^{(r)}$ may be replaced by the complex analytic signal[23]

$$\vec{E}(\vec{r},\, t) = \int_{-\infty}^{\infty} \vec{V}(\vec{r},\, \omega)\, e^{-i\omega t}\, d\omega \tag{38}$$

The probability of photoelectron emission from a detector that is illuminated by the field (equation 38) is given by

$$p_1(t)\delta t = \sigma \langle \vec{E}^*(t) \cdot \vec{E}(t) \rangle\, \delta t \tag{39}$$

where $\vec{E}^*(t) \cdot \vec{E}(t)$ is the instantaneous intensity, and σ is the quantum efficiency. The dependence of $p_1(t)\delta t$ on $\vec{r}$ has been suppressed on the assumption of spatial coherence at the detector.

The joint probability, $p_2(t_1, t_2)\, \delta t_1\, \delta t_2$, of registering two photocounts at times t_1 and t_2 within δt_1 and δt_2 is[10,19,22]

$$p_2(t_1, t_2)\delta t_1\, \delta t_2 = \sigma^2 \langle [\vec{E}^*(t_1) \cdot \vec{E}(t_1)][\vec{E}^*(t_2) \cdot \vec{E}(t_2)] \rangle\, \delta t_1\, \delta t_2 \tag{40}$$

For a stationary field, the average depends only on the time interval between pulses, $\tau = t_2 - t_1$ (figure 3). Therefore,

$$p_2(t_1, t_1 + \tau)\, \delta t_1\, \delta \tau = \bar{n}^2 C^{(2)}(\tau)\delta t_1\, \delta \tau \tag{41}$$
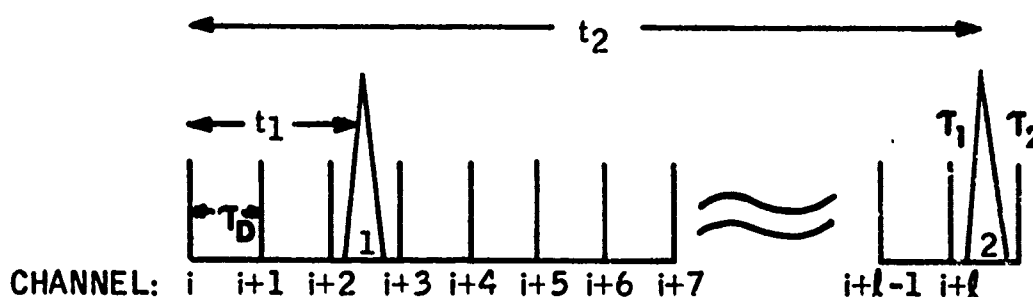

Figure 3. Pulse Interval Analysis Scheme

[22]Glauber, R. J. The Quantum Theory of Optical Coherence. Phys. Rev. 130, 2529 (1963).
[23]Born, M., and Wolf, E. Principles of Optics. 3d Ed. Pergamon Press, Oxford, England. 1966.

16

where the normalized second-order correlation coefficient is given by

$$C^{(2)}(\tau) = \frac{\langle [\vec{E}^*(t_1) \cdot \vec{E}(t_1)] [\vec{E}^*(t_1 + \tau) \cdot \vec{E}(t_1 + \tau)] \rangle}{\langle \vec{E}(t) \cdot \vec{E}(t) \rangle^2} \qquad (42)$$

and $\dot{n}$ = mean count rate of the illuminated detector. For Gaussian random fields, the normalized second-order correlation function, $C^{(2)}(\tau)$ is related to $C^{(1)}(\tau)$ by[5,13]

$$C^{(2)}(\tau) = [\ 1 + |C^{(1)}(\tau)|^2] \qquad (43)$$

where $C^{(1)}(\tau)$ is now the normalized version of equation 26,

$$C^{(1)}(\tau) = e^{-D|\vec{K}|^2|\tau|} e^{-i\omega_o \tau} \qquad (44)$$

Equation 41 assumes that all counts registered are a result of the absorption of photons at the detector surface. In practice, the dark current is responsible for a mean residual count rate, $\dot{m}$, which is unrelated to the incident radiation. Equation 41 must, therefore, be modified to read[19]

$$p_2(t_1, t_1 + \tau)\delta t_1 \delta\tau = [(\dot{n}^2 + \dot{m}^2) + \dot{n}^2 |C^{(1)}(\tau)|^2]\ \delta t_1 \delta\tau \qquad (45)$$

The number of pulse pairs, N, that will be counted with a time increment τ within the range $\tau_1 \leqslant \tau \leqslant \tau_2$ is given by

$$N(\tau_1, \tau_2) = t_s \left[(\dot{n}^2 + \dot{m}^2)(\tau_2 - \tau_1) + \dot{n}^2 \int_{\tau_1}^{\tau_2} |C^{(1)}(\tau)|^2\ d\tau \right] \qquad (46)$$

where t_s = the total sampling time.

The first term inside the brackets of equation 46 gives the random rate of pulse pair production, which is constant so long as $(\tau_2 - \tau_1)$ is unchanged; the second term represents the "excess" counting rate produced by the bunching phenomenon. The bunching term will contribute significantly only when $\tau \lesssim \tau_c$, because $|C^{(1)}(\tau)|$ (equation 44) is small for values of τ that are appreciably larger than τ_c. For this reason, the upper limit τ_2 in the integral (equation 45) may be approximated by $\tau_2 = \infty$ so that

$$\int_{\tau_1}^{\infty} |C^{(1)}(\tau)|^2\ d\tau = 1/2D|\vec{K}|^2 e^{-2D|\vec{K}|^2|\tau_1|} \qquad (47)$$

Applying this result to equation 46 gives

$$N(\tau_1) = t_s[(\dot{n}^2 + \dot{m}^2)(\tau_2 - \tau_1) + \dot{n}^2/2\delta\omega e^{-2\delta\omega|\tau_1|}] \qquad (48)$$

According to equation 48, a determination of the number of two pulse counts as a function of τ_1 will provide a method of measuring the half width of the spectrum, $\delta\omega$. Furthermore, because the time resolution requires decreases as $\delta\omega$ becomes smaller, this method of spectrum analysis becomes very attractive for narrow spectral lines such as the scattered light from particles undergoing translational diffusion.

17

V.   APPARATUS AND PROCEDURES.

A block diagram of the laboratory experiment is shown in figure 1. This apparatus allows us to measure the half width at half height, $\delta\omega$, of the scattered light by determining the number of two pulse counts as a function of τ_1 (equation 48). The experimental equipment consisted of (see also appendix A) the following.

A.   Laser.

A helium-neon laser with an output of 10^{-3} watts at 632.8 nm. The laser beam is polarized perpendicular to the scattering plane.

B.   Lens.

A lens of 7.5-cm focal length was used to focus the laser beam in the sample cell. It is desirable to do this because the number of coherence areas (see paragraph D) in a given solid angle decreases as the scattering volume decreases.

C.   Sample.

A spectrophotometer cell of dimensions 1.0 by 1.0 by 4.7 cm was used to hold the sample. The sample was prepared by diluting the polystyrene emulsion with distilled water until no halo effect from secondary scattering could be observed. Because 0.557-μm spheres are strong forward scatterers,[7] there was no difficulty in eliminating the secondary scattering while maintaining a strong scattered beam at an angle of 30°.

D.   Aperture Stops A and B.

The purpose of the aperture stop A was twofold: (1) to prevent any stray light scattered from the edges of the sample cell from reaching the photocathode; and (2) to provide a narrow beam of the scattered light with a well-defined scattering angle. The aperture A was circular with a diameter of 0.0711 cm.

The aperture B was located at a distance of 45 cm from the sample cell. The size of this aperture is of .·· .portance because the detector area must be limited to that area over which the optical field is spatially coherent (see page 12) i.e., the area of coherence. Detector areas larger than the area of coherence will produce pulses that will be correlated with each other in random fashion. Cummins and Swinney[13] give a detailed calculation of the area of coherence* for a quasi-monochromatic source that shows that for a single coherence area, the detector area should be

$$A \ll \lambda^2/\Omega \qquad (49)$$

where Ω = the solid angle that the source subtends at the detector. For this experiment aperture B was circular with a diameter of 0.0711 cm, which gives

$$A(\lambda^2/\Omega)^{-1} \approx 0.53 \qquad (50)$$

---

*See also Mandel and Wolfe;[10] Forrester, Gudmundsen, and Johnson;[11] and Forrester.[24]

[24] Forrester, A. T. On Coherence Properties of Light Waves. Amer. J. Phys. 24, 192 (1956).

18

E.   Photomultiplier and High Voltage Supply.

The photomultiplier tube (PMT) in this experiment was an RCA type 6217.[25,26] The S-10 spectral response of the photocathode of the 6217 PMT produces good quantum efficiency, $\sigma \approx 0.013$, in the spectral region of 632.8 nm; the 10 dynodes produce a current gain of $G \approx 3 \times 10^5$ when the cathode-anode voltage is 900 volts. The electronic circuitry associated with the PMT is shown in figure 4.

The high voltage power supply is capable of providing approximately 1 ma of current to the dynode chain when the voltage drop across the PMT is 900 volts. The high voltage is passed through a π-section RC filter network before it is applied to the PMT. The purpose of the filter is to prevent the incoming a.c. components in the high voltage from appearing as an output voltage across R. The ripple factor for this filter is given by[27]
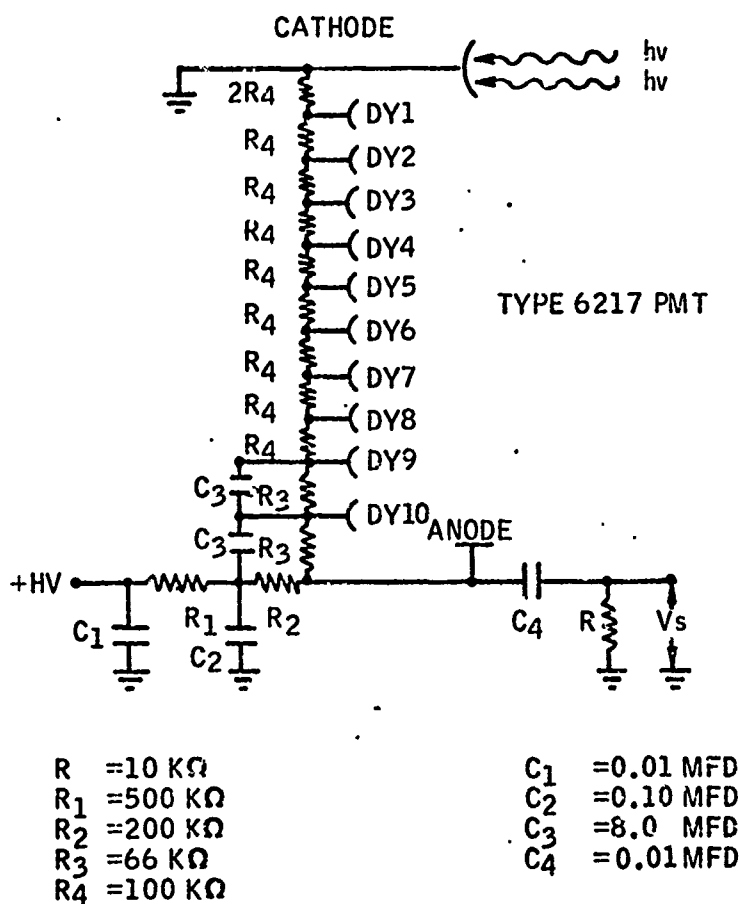

R =10 KΩ	C_1 =0.01 MFD
R_1 =500 KΩ	C_2 =0.10 MFD
R_2 =200 KΩ	C_3 =8.0 MFD
R_3 =66 KΩ	C_4 =0.01 MFD
R_4 =100 KΩ	

Figure 4. Photomultiplier Circuitry

[25]Photomultiplier Tubes for New Equipment Design. Radio Corporation of America, Harrison, New Jersey. 1967.

[26]RCA 6217 Multiplier Phototube Data Sheet. Radio Corporation of America, Harrison, New Jersey. 1959.

[27]Malmstadt, H. V., Enke, C. G., and Toren, E. C. Electronics for Scientists. W. A. Benjamin, Inc., New York, New York. 1963.

$$r.f. = 10^{-5}/C_1 C_2 R_1 R_L \approx 0.015 \tag{51}$$

where R_L = total resistive load following the filter section. The resistor, R_2, serves to isolate the pulses appearing at the anode from the filter section, whereas the capacitor, C_4, isolates the high voltage d.c. from the output.

The output pulses from the PMT that appear at the anode are integrated on the stray capacitance, C, which appears at the output (figure 5a). Let us consider the interaction of an idealized pulse (figure 5b):

$$i_0 = 0, \qquad 0 > t > T$$

$$i_0 = i_1 + i_2, 0 < t < T \tag{52}$$

with this circuit. The resulting voltage output is given by (see figure 5c),

$$V_s(t) = 1/C \int_0^t i_1 dt = i_2 R = i_0 R(1 - e^{-t/RC}), 0 < t < T \tag{53}$$

and

$$V_s(t) = v_0 e^{-t/RC}, t > T \tag{54}$$

The magnitude of the stray capacitance is on the order of 100 pf so that $RC \approx 10^{-6}$ second. Because $T/RC \approx 10^{-6}$, a first-order expansion of equation 52 may be used to find the maximum voltage developed by the pulse

$$V_0 = Ge/C \approx 5 \times 10^{-4} \text{ volts} \tag{55}$$

where e = electron charge. Therefore, the output pulses of the PMT will have a duration of approximately 1 μsec and a maximum voltage of about 0.5 (mV).

F.   Amplifier.

The multichannel analyzer accepts pulses of 0 to 2 volts with a duration of approximately 1 μsec at the direct access connector. The selection of $R = 10K\Omega$ stretches the pulses to the required time duration, but amplification on the order of 10^3 to 10^4 is required to raise the voltage to the desired level.

A pulse amplifier circuit (figure 6) was constructed on a model RP operational manifold.[28] This manifold is provided with plug-in receptacles that accept up to eight operational amplifiers. A color-coded jack field, which permits the installation and interconnection of circuit elements, and a regulated d.c. power supply are an integral part of the manifold. Four amplifier stages, each employing a model EP85AU amplifier,[27] were constructed in a simple inverting configuration. The unity gain crossover point for these amplifiers is about 2 MHz; because no provision is made for changing the internal compensation of these amplifiers, amplification by successive stages was used to preserve as much bandwidth as possible.

---

[28]Philbrick Model RP Operational Manifold. Philbrick Researches, Dedham, Massachusetts. 1967.
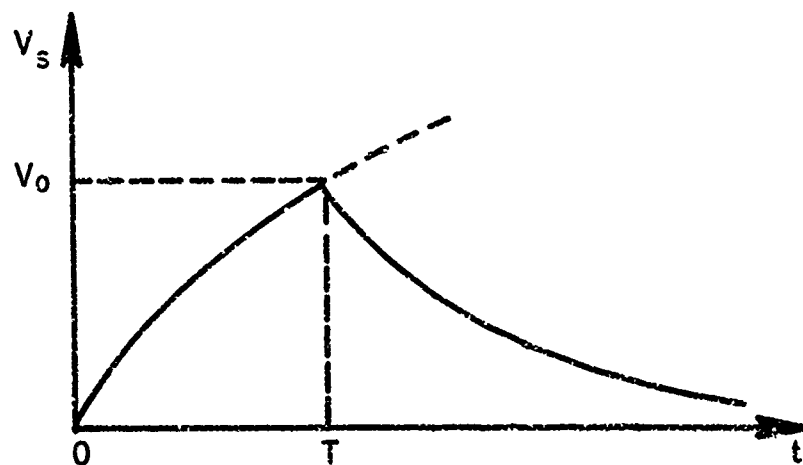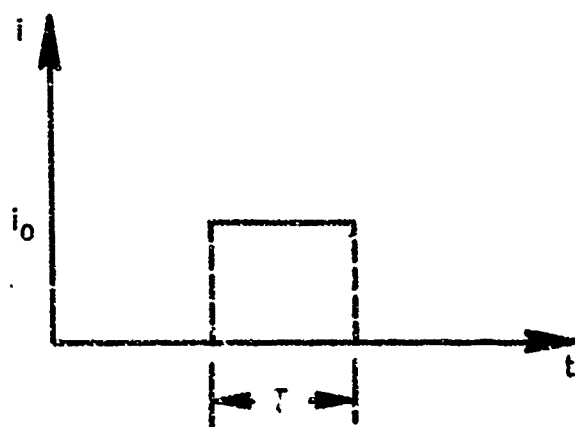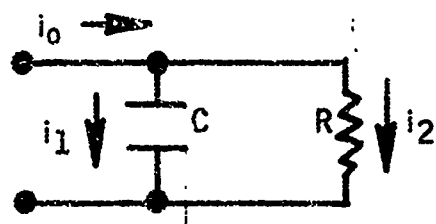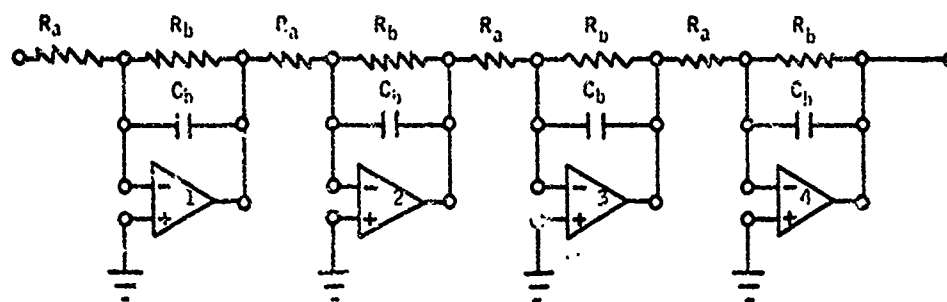
Figure 5. Pulse Output Circuitry

EP85AU OPERATIONAL AMPLIFIERS

$R_a = 10K\Omega$ $C_b = 100\,pf$

$R_b = 100K\Omega$ $G = (R_b/R_a)^4 = 10^4$

Figure 6. Pulse Amplifier Circuit

The performance of the amplifier circuit was checked by inputing the calibrated square wave from an oscilloscope. The square wave inputs were 0.5 mV and 0.2 mV PTP and had a frequency of 10^3 Hz. The amplified square wave pulses were observed on the oscilloscope, and the predicted gain of 10^4 was verified. Some distortion in the form of narrowing and rounding of the square wave was noted. Amplified dark current pulses from the PMT were also observed on the oscilloscope and found to have peak voltages of just under 2 volts.

G.   Multichannel Analyzer.

The multichannel analyzer (MCA) has 127 channels that are available to count voltage pulses, and it has the ability to store the counts in memory for later retrieval. In this experiment the MCA was used in the multiscaling mode in which each channel will accept counts for a certain preselected dwell time and then transfer to the next channel until all 127 channels have been sampled. Figure 3 illustrates the way in which the time interval τ_1 associated with a 2-pulse count is determined. It is easily seen that

$$\tau_1 = l\tau_c \tag{56}$$

where τ_c = the dwell time. For the 0.557-μm polystyrene spheres, the coherence time for a scattering angle of $30°$ is $\tau_c \approx 27$ ms. Therefore, it was necessary to employ the shortest dwell time available on the MCA, 1 ms, to execute the experiment.

For the observation of the spectrum of the scattered light, the apparatus was assembled as shown in figure 1. To facilitate optical alinement of the apparatus, the lens, sample cell, and apertures A and B were mounted on small laboratory jacks. The operational amplifiers were balanced in accordance with the manufacturer's instructions,[28] and the balancing procedure was repeated at half-hour intervals during the course of the experiment. The scattering angle was set by making the distance from the center of sample cell to the PMT equal to 45 cm (±1 cm), and the distance from the PMT to the center of the direct laser beam was made equal to 27.5 cm (±1 cm). The concentration of the polystyrene spheres was then adjusted so that single pulses were being counted by the MCA. The output of the PMT was scanned with the MCA a total of 35 times. At the end of each scan, which required approximately 127 ms, a record of the data was created by reading

22

the memory of the MCA out through a teletypewriter. A similar set of data was produced for dark current pulses by blocking aperture B and recording the data as described earlier.

VI. RESULTS AND CONCLUSIONS.

The data for the scattered light and the dark current were analyzed according to the scheme presented in Section V. The results of the analysis are presented in figures 7 and 8.

For the scattered light an estimate for the optical linewidth, $\delta\omega$, was obtained by a least-squares fit of the experimental data to the function (see appendix B).

$$N = A + Be^{\alpha\tau_1} \tag{57}$$

where

$$\alpha = -2\delta\omega$$

The parameters A and B depend on the sample time, linewidth, detector area, and dead time effects. The usual procedure of treating A and B as independent parameters has been followed in obtaining this fit.[29] The least-square fit gives
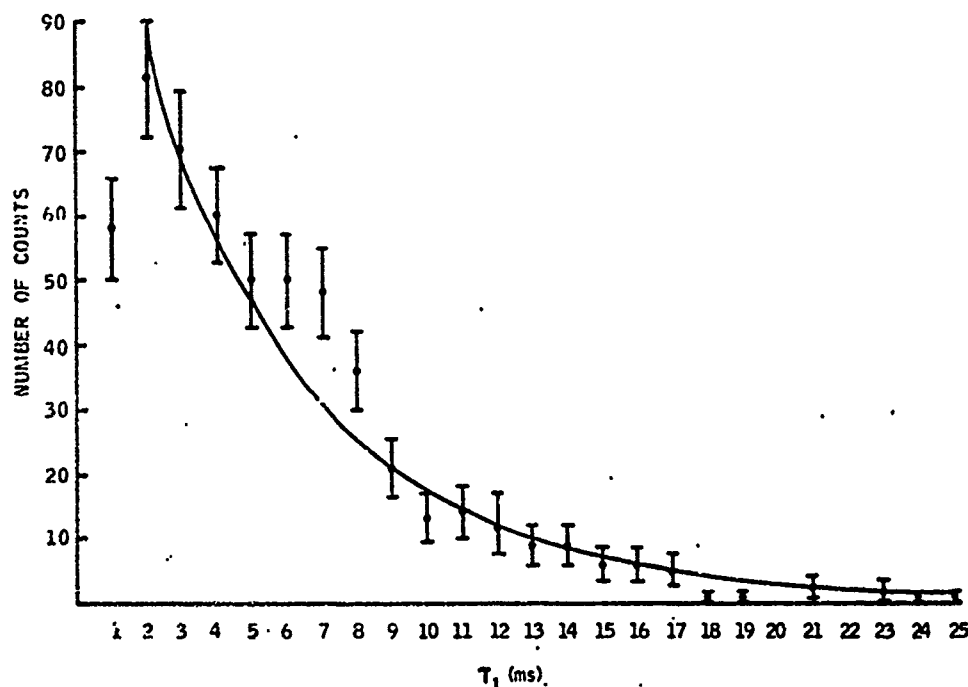
$$\delta\omega = 102 \text{ Hz} \tag{58}$$

Figure 7. Spectral Data

---

[29]Jakeman, E., Pike, E. R., and Swain, S. Statistical Accuracy in the Digital Autocorrelation of Photon Counting Fluctuations. J. Phys. A: Gen. Phys. 3, 155 (1970)
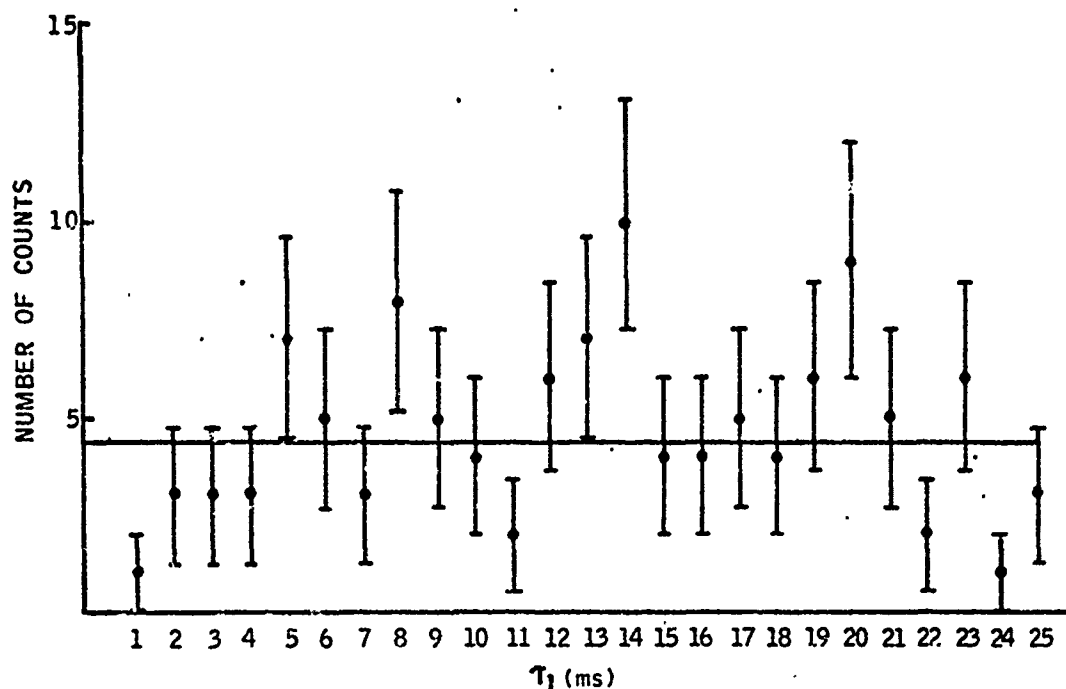
Figure 8. Dark Current Data

which yields a value for the diffusion constant of

$$D = 3.23 \times 10^{-7} \, cm^2/sec \qquad (59)$$

The linewidth as determined experimentally is considerably larger than predicted by equation 30, which gives, $\delta\omega \approx 37$ Hz. This excess broadening is attributed to the presence of nonuniform convection currents by Cummins, Knabler, and Yeh,[9] whose data for 0.557-μm spheres are in substantial agreement with the results found herein. Because no attempt was made to isolate the sample thermally and acoustically, some improvement in the results may be possible. The use of particles of smaller size would render the effect of convection broadening relatively less important, but the time resolution required to perform the experiment would be increased.

The results obtained from the dark current pulses (figure 8) are in agreement with the prediction of equation 48, that the random rate of pulse pair production is constant so long as ($\tau_2 - \tau_1$) is unchanged. Therefore, the excess coincidence found for the scattered light may be attributed to the motion of the scatterers, not to any unusual characteristics of the dark current pulses.

In conclusion, then, we have seen how the diffusive motion of scatters in dilute suspension produces a well-defined spectrum in the scattered light. It was shown that the technique of pulse interval analysis provides a method of recovering information about the motion of the scatterers from such a spectrum. Finally, an experiment to measure the spectrum of the scattered light was designed and executed. The results of this experiment yielded a spectral linewidth that was caused not only by diffusive motion, but also by the convective motion of the scatterers. This determination of the linewidth was found to be in agreement with previous experimental results.

24

For our purposes, the main interest in such light-scattering studies stems from their potential application to particle sizing problems. From equation 30 it can be seen that for a fixed scattering angle, a determination of the optical linewidth enables one to find the Stokes diameter of the particles. However, many problems—such as the effects of polydispersity on the spectral width, and the convective motion of the particles—must be solved before this technique becomes practical.

LITERATURE CITED

1. Fuchs, N. A. The Mechanics of Aerosols. The Macmillan Company, New York, New York. 1964.

2. Einstein, A. Investigations on the Theory of the Brownian Movement. ed R. Furth. Dover, New York, New York. 1956.

3. Chandrasekhar, S. Stochastic Problems in Physics and Astronomy. Rev. Mod. Phys. *15*, 1 (1943).

4. Wang, M. C, and Uhlenbeck, G. E. On the Theory of the Brownian Motion II. Rev. Mod. Phys. *17*, 323 (1945).

5. Clark, N. A., Lunacek, J. H., and Benedek, G. B. A Study of Brownian Motion Using Light Scattering. Amer. J. Phys. *38*, 575 (1970).

6. Van De Hulst, H. C. Light Scattering by Small Particles. John Wiley & Sons, New York, New York. 1957.

7. Ashley, L. E., and Cobb, C. M. Single Particle Scattering Functions for Latex Spheres in Water. J. Opt. Soc. Amer. *48*, 261 (1958).

8. Korn, G. A., and Korn, T. A. Mathematical Handbook for Scientists and Engineers. McGraw Hill, New York, New York. 1961.

9. Cummins, H. Z., Knable, N., and Yeh, Y. Observation of Diffusion Broadening of Rayleigh Scattered Light. Phys. Rev. Lett. *12*, 150 (1964).

10. Mandel, L., and Wolf, E. Coherence Properties of Optical Fields. Rev. Mod. Phys. *37*, 231 (1965).

11. Forrester, A. T., Gudmundsen, R. A., and Johnson, P. O. Photoelectric Mixing of Incoherent Light. Phys. Rev. *99*, 1961 (1955).

12. Forrester, A. T. Photoelectric Mixing as a Spectroscopic Tool. J. Opt. Soc. Amer. *51*, 253 (1961).

13. Cummins, H. Z., and Swinney, H. L. Progress in Optics. Vol VIII. ed E. Wolf. John Wiley & Sons, New York, New York. 1970.

14. Jakeman, E., and Pike, E. R. The Intensity-Fluctuation Distribution of Gaussian Light. J. Phys. A, Proc. Phys. Soc. (London) *1*, 128 (1968).

15. Mandel, L., and Wolf, E. Comments on a Paper by E. Jakeman and E. R. Pike, 'The Intensity-Fluctuation Distribution of Gaussian Light.' J. Phys. A, Proc. Phys. Soc. (London) *1*, 625 (1968).

16. Jakeman, E., Oliver, C. J., and Pike, E. R. A Measurement of Optical Linewidth by Photon-Counting Statistics. J. Phys. A, Proc. Phys. Soc. (London) *1*, 406 (1968).

17. Arrecchi, F. T., Berné, A., and Sona, A. Measurement of the Time Evolution of a Radiation Field by Joint Photocount Distributions. Phys. Rev. Lett. *17*, 260 (1966).

18. Bédard, G. N-Fold Joint Photon Counting Distributions Associated with the Photoelection of Gaussian Light. Phys. Rev. *161*, 1304 (1967).

19. Morgan, B. L., and Mandel, L. Measurement of Photon Bunching in a Thermal Light Beam. Phys. Rev. Lett. *16*, 1012 (1966).

20. Phillips, D. T., Kleiman, H., and Davis, S. P. Intensity-Correlation Linewidth Measurement. Phys. Rev. *153*, 113 (1967).

21. Pusey, P. N., and Goldburg, W. I. Temperature Dependence of Concentration Fluctuations in a Binary Liquid Mixture Using a Photon Correlation Method. Appl. Phys. Lett. *13*, 321 (1968).

22. Glauber, R. J. The Quantum Theory of Optical Coherence. Phys. Rev. *130*, 2529 (1963).

23. Born, M., and Wolf, E. Principles of Optics. 3d Ed. Pergamon Press, Oxford. England. 1966.

24. Forrester, A. T. On Coherence Properties of Light Waves. Amer. J. Phys. *24*, 192 (1956).

25. Photomultiplier Tubes for New Equipment Design. Radio Corporation of America, Harrison, New Jersey. 1967.

26. RCA 6217 Multiplier Phototube Data Sheet. Radio Corporation of America, Harrison, New Jersey. 1959.

27. Malmstadt, H. V., Enke, C. G., and Toren, E. C. Electronics for Scientists. W. A. Benjamin, Inc., New York, New York. 1963.

28. Philbrick Model RP Operational Manifold. Philbrick Researches, Dedham, Massachusetts. 1967.

29. Jakeman, E., Pike, E. R., and Swain, S. Statistical Accuracy in the Digital Autocorrelation of Photon Counting Fluctuations. J. Phys. A: Gen. Phys. *3*, 155 (1970).

APPENDIXES

APPENDIX A

EQUIPMENT AND MATERIALS LIST

1. Laser. Spectra Physics Model 132-01. Spectra-Physics Inc., Mountain View, California.

2. Sample. Polystyrene Latex: 0.557 μm. Bioproducts Department, The Dow Chemical Company, Midland, Michigan.

3. Sample Cell. Opticell Spectrophotometer Cell. Optical Cell Company, Inc., Brentwood, Maryland.

4. Photomultiplier. RCA 6217. Radio Corporation of America, Harrison, New Jersey.

5. Power Supply. Atomic Power Supply. Model 316, Positive.

6. Amplifier. Philbrick Model RP Operational Manifold, Operational Amplifiers: Model EP85AU. Philbrick Researches, Dedham, Massachusetts.

7. Multichannel Analyzer. Nuclear Data Model ND-110. Nuclear Data, Inc., Schaumburg, Illinois.

8. Oscilloscope. Tektronix Type 545. Tektronix, Inc., Beaverton, Oregon.

9. Laboratory Jack. Little Jack. Precision Scientific Co., Chicago, Illinois.

APPENDIX B

LEAST-SQUARES FIT OF EXPERIMENTAL DATA

In order to fit a least-squares curve to the experimental data, the equation (equation 48 in text)

$$N(\tau_1) = t_s \left[(\dot{n}^2 + \dot{m}^2)(\tau_2 - \tau_1) + \dot{n}^2/2 \, \delta\omega e^{-2\omega|\tau_1|} \right]$$

is rewritten as

$$(N - A) = Be^{\alpha\tau_1} \qquad (1B)$$

where $\alpha = -2\delta\omega$, and A and B are regarded as independent parameters. Equation 1B is then transformed to the linear form

$$\ln(N - A) = \ln B + \alpha\tau_1 \qquad (2B)$$

in order to carry out the least-squares analysis.

Because equation 2B involves three parameters (A, B, α), the best fit is obtained by making successive estimates of A and calculating B and α in the usual manner. The Gauss criterion* is employed to determine the set of parameters that give the best fit in the least-squares sense. This criterion states that the best fit is obtained when the quantity

$$\xi = \frac{\sum_i d_i^2}{n - m} \qquad (3B)$$

where

d_i = deviation of the measured y values from the computed values

r = number of observed data pairs

m = number of free parameters

is minimized.

Figure B shows ξ plotted as a function of the estimated values of A. It is readily seen by inspection that the minimum of ξ occurs when $A = 1.00$. The corresponding least-squares fit is

$$N = 1.00 + 125e^{-0.203\tau_1} \qquad (4B)$$

where τ_1 is in units of milliseconds.

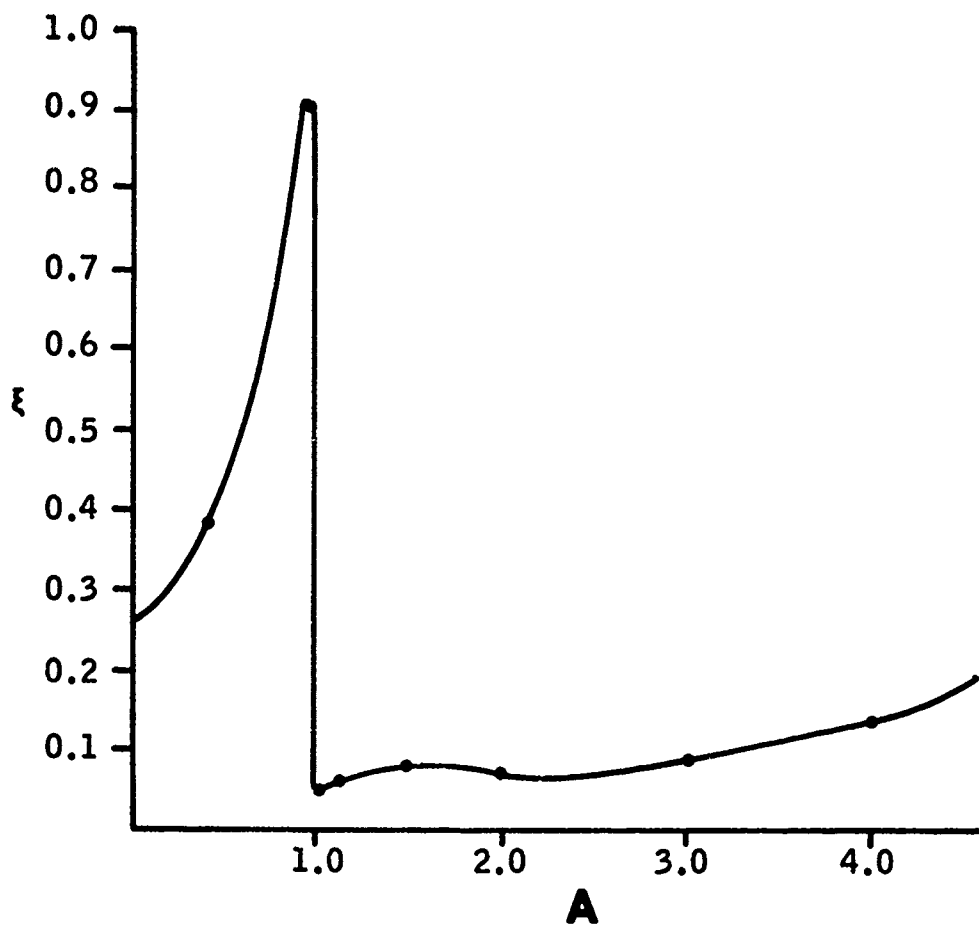*Worthing, A. G., and Geffner, J. Treatment of Experimental Data. John Wiley & Sons, New York, New York. 1950.

Figure B. Minimization of the Gauss Criterion